

IMPROVEMENTS IN THE CHARACTERIZATION OF PHOSPHATE DEPOSITS USING WELL LOGGING IN THE TAPIRA ALKALINE-CARBONATITE COMPLEX, MINAS GERAIS, BRAZIL

Caio de Almeida Paula  , Caio Almeida Carvalho  ,

Marco Antônio Braga  , Patrick Führ Dal' Bó  , Viktor Souto Louback  ,

Paulo Salvadoretti  , Leonardo Braga Vieira  , Laura Carolina Oliveira Paes  ,

Rodolfo B. de Oliveira Gonçalves  , Lucas David Feuchard  , and Kliver Peixoto Santos  

¹Universidade Federal do Rio de Janeiro - UFRJ, Centro de Pesquisa em Geofísica Aplicada - CPGA, Rio de Janeiro, RJ, Brazil

²Universidade Federal do Rio Grande do Sul - UFRGS, Porto Alegre, RS, Brazil

³Mosaic Fertilizantes do Brasil SA, Tapira, MG, Brazil

*Corresponding author e-mail: caio@geologia.ufrj.br

ABSTRACT. Well logging is an effective tool for the investigations of the subsurface, especially in the exploration of mineral deposits. This method was applied to five boreholes at the Tapira Mining Complex in Minas Gerais state, Brazil, where phosphate is mined in the supergene mantle of an alkaline-carbonatite intrusion. The objective of this study is to acquire bulk density (gamma-gamma) and natural gamma data through geophysical well logging, processing and analyzing them to define the intervals of interest for mining and comparing them with the traditional density acquisition method. The equipment used included a probe for density and natural gamma, a caliper and acoustic/optical televiewers; they provided measurements of borehole density, radioactivity, diameter and visual details for analysis. Following the caliper data, the boreholes were predominantly well preserved, which contributed to the measurements of geophysical parameters. The density logs showed a compartmentalized pattern with three well-defined intervals in the five boreholes, which were associated with weathering horizons. The natural gamma logs also exhibited intervals with higher measurements related to the boundaries between horizons. Televiewers allowed the observation of weathering effects along some of the boreholes. Based on the data analysis, it was possible to delineate the mineralized interval within the weathered mantle with density around 1.9 - 2.2 g/cm³ and correlate it among all drill holes. Compared to the traditional laboratory analysis, geophysical logging proved to be a more consistent and reliable method to measure density that is less susceptible to external interferences.

Keywords: Wireline logging gamma-gamma density log mineral exploration agrominerals.

INTRODUCTION

Geophysics plays a crucial role in mining, especially in the exploration of mineral deposits, by providing indirect data about the subsurface when direct methods are not easily applied (Silva and Luiz, 1995; Mussett and Khan, 2000; Luiz, 2013). Geophysical logging consists of recording

a geophysical parameter of the rock along a borehole, this technique is widely used in oil & gas and can also be applied in mineral exploration. Wireline well logging probes can be used to measure various physical properties, through mechanical, spontaneous, and induced measurements. The method offers high-resolution measurements compared to direct methods applied to drill core samples, provides results in less time, and also reduces uncertainty due to being an in situ measurement (Ellis and Singer, 2008; Silva, 2010; Rider and Kennedy, 2011; Nery, 2013; Reis et al., 2021).

Works related to coal exploration are the most common and yield results that meet the optimization needs for deposit investigation (Kowalski and Fertl, 1977; Oliveira, 2005; Webber, 2008; Souza et al., 2010; Webber et al., 2013; Gasper et al., 2015; Horrocks et al., 2015; Gorelik et al., 2019). In Brazil, geophysical logging has also been employed in exploratory activities for iron ore, enhancing the efficiency of the process (Almeida, 2011; Fonseca, 2014; Pereira et al., 2016a; Pereira et al., 2016b; Prieto, 2021). Logging data is already used in the prospecting of uranium deposits (Howell et al., 1980; Penney et al., 2012; Hajnal et al., 2015; Carasco et al., 2018), as well as in phosphate deposits (Wynn, 1996; Asfahani and Abdul-Hadi, 2001; Asfahani, 2002; Asfahani, 2019)

The Tapira Alkaline-Carbonatite Complex is an ultramafic alkaline-carbonatite intrusion which is part of Alto Paranaíba Igneous Province (APIP), characterized by containing phosphate-rich rocks (Gibson et al., 1995; Brod et al., 2004; Gomes, 2020). The Tapira Mining Complex (TMC) is located in Tapira municipality, west of Minas Gerais State. TMC is among the largest phosphate producers in Brazil for the production of fertilizers and mining is focused on the supergene mantle, operating since the 1970s (Conceição and Bonotto, 2006; Conceição et al., 2022). In the current scenario, Brazil still depends on external production for its fertilizer supply, therefore it becomes highly important to implement actions that optimize phosphate production to meet this demand and reduce external dependence (Abram et al., 2011; 2016; ANM, 2019; Brasil, 2021; 2023).

Bulk density is a critical component in mineral resource investigations as it enables the estimation of mineralized volumes. The factors such as weathering, alteration type, lithology, and ore mineral assemblage are associated with variations in density measurements (CIM, 2018; 2019). Subsurface investigations in the TMC are carried out through the lithological description of drilling cores and the measurement of core sample density using the hydrostatic balance method water displacement (Lipton, 2001; Lipton and Horton, 2014). However, this type of procedure faces challenges due to the condition of the drill core samples. These samples are generally unconsolidated, making it difficult to determine the rock density accurately and potentially leading to results that are inconsistent with reality.

This study aims to acquire, process and interpret geophysical logs, including density, natural gamma, caliper, and imaging logs, from five boreholes in the Tapira Mining Complex. Four geophysical probes were used, with the primary tool dedicated to acquiring bulk density

and natural gamma logging, these two parameters are the most effective in investigating the weathering mantle of the Tapira Alkaline-Carbonatite Complex and its phosphate-mineralized horizon.

Density, natural gamma, and caliper data were collected in all boreholes, except for televiewers. The density logs obtained were compared to laboratory density test results and used to identify the mineralized weathering horizon with the assistance of caliper and natural gamma logs. The logs enabled the determination of the economically significant interval for phosphate mining as well as its spatial distribution, and compared to laboratory analyzes, the results were more coherent and reliable.

The geophysical method was able to refine the delimitation of the mineralized interval and reported notable differences in density compared to the traditional methodology. These differences can impact directly on the evaluation of phosphate reserves. Therefore, geophysical data can be applied to the ore volumes estimation and mine planning in a faster, safer, and more reliable manner than traditional methods.

GEOLOGICAL SETTINGS

The Alto Paranaíba Igneous Province is an alkaline province located on the northeastern margin of the Paraná Basin and southwest portion of the São Francisco Craton (Gibson et al., 1995). This province originated alkaline-carbonatite complexes from mafic-ultramafic and ultrapotassic magmatic events that caused the formation of intrusive bodies in Neoproterozoic rocks, creating dome-like structures. These complexes are located in the state of Goiás and Minas Gerais and are referred as Catalão I, Catalão II, Serra Negra, Salitre, Araxá, and Tapira (Oliveira et al., 2004; Gomes, 2020).

The Tapira Alkaline-Carbonatite Complex is the southern most complex in the province, and its rocks have been dated by Sonoki and Garda (1988) to the Late Cretaceous, with ages ranging from 87.2 to 85.6 Ma. The complex covers an approximate area of 35 km² in an elliptical shape and is intruded into the rocks of the Canastra Group (Barbosa et al., 1970; Bezerra and Brod, 2013). Among the rocks of the Tapira Complex, the bebedouritic series is predominant, represented by two lithotypes from different intrusions in an association of serpentized dunite, carbonatite, syenite, metasomatic phlogopitite, and ultramafic-potassic dikes. The carbonatite series, which is also present, is divided into five units that differ in composition, along with a syenitic intrusion (Brod et al., 2013; Gomes, 2020).

Phosphate is the main ore mined in the Tapira Mining Complex, found in residual concentrations in the lateritic cover with thickness from 70 to 120 m. The mineral group is represented by apatite, which is important in this context because the development of the general mineralization model is directly conditioned by the action of weathering. This factor is increased by the centripetal drainage pattern and is concentrated in the complex because the host rocks are more resistant (Bezerra and Brod, 2013). The phosphate deposits are normally

associated with portions of evolved bebedourites, where the mining is concentrated.

The weathering process favors the formation of the thick lateritic cover, contributing to the supergene enrichment of phosphate. In this model, weathering horizons are considered, which differ from each other by the phosphate content, from bottom to top: fresh rock, saprolite poorly concentrated in phosphate, a phosphatic horizon, a zone rich in TiO_2 , and topmost a soil cover (Figure 1) (Conceição and Bonotto, 2006; Conceição et al., 2022). TMC is the main phosphate mining unit in Brazil, holding the first position in ore volume in the country and the second in the world, and all this potential is directed towards the production of fertilizers (Abram et al., 2016).

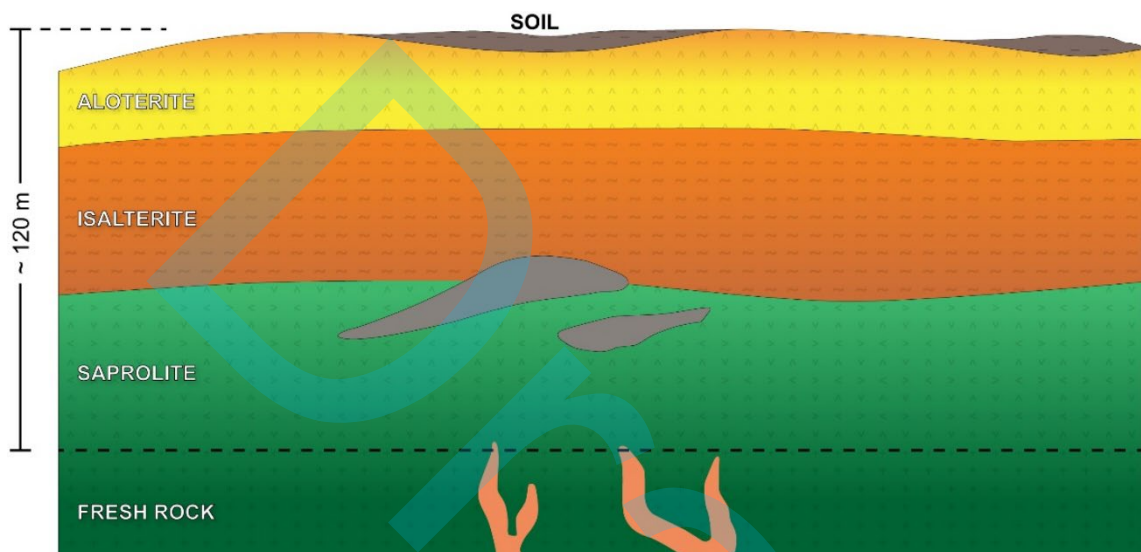


Figure 1: Schematic model of the lateritic profile of phosphate mineralization in the Tapira Mining Complex. (Adapted from Conceição and Bonotto, 2006; Novaes, 2018).

METHODS

The geophysical data acquisition operation was carried out by a winch that pulls the probe up through a cable which, in addition to supporting the probe, also transmits the parameter's measurements to an interface that converts them into digital data that can be read by a connected computer, allowing real-time monitoring of the recording. In this system, a pulley positioned above the borehole is used to measure the depth metrically and determine the acquisition speed (Ellis and Singer, 2008; Nery, 2013).

The well logging campaign was carried out in five boreholes, previously drilled with a diameter of 96.3 mm, within the Tapira Mining Complex, located approximately 400 km west of Belo Horizonte, in the Tapira municipality. The operation at the mining complex was carried out in boreholes with a depth from 50 to 120 m, using the standard procedure for wireline well logging (Figure 2). Prior to the acquisition phase, all equipment underwent their respective calibration processes at the Centro de Pesquisa em Geofísica Aplicada – Universidade Federal do Rio de Janeiro (CPGA-UFRJ).

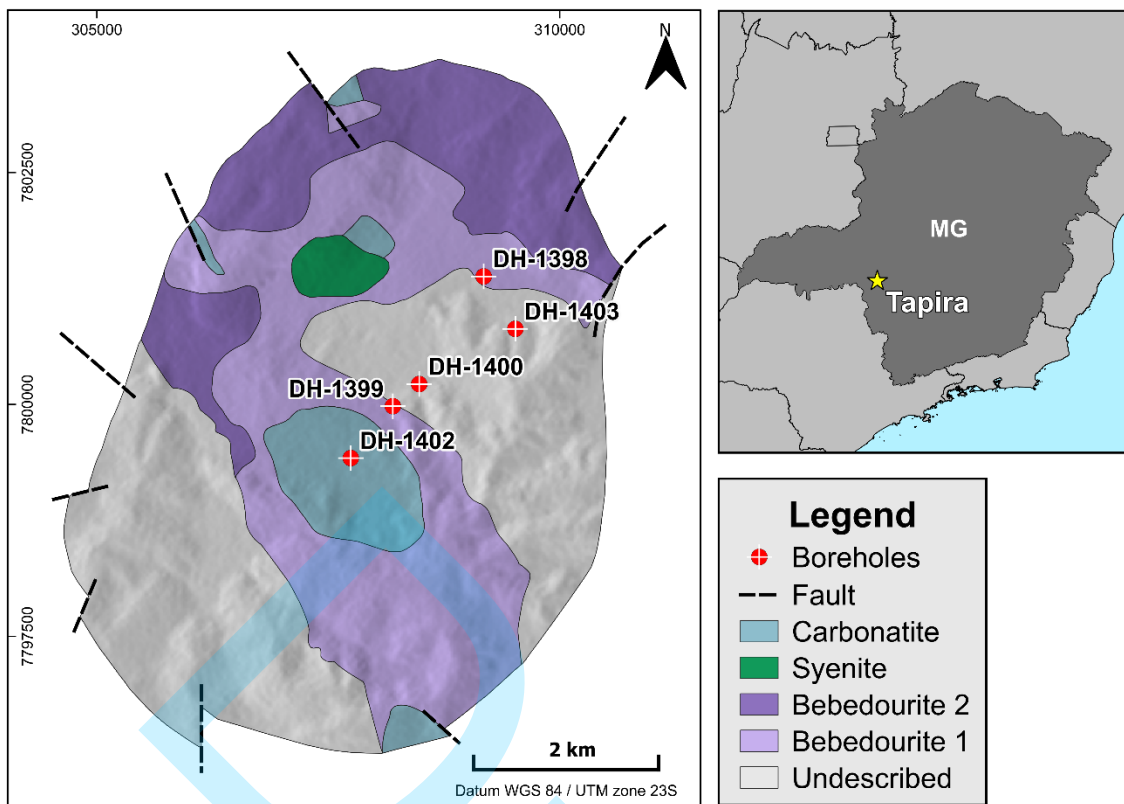


Figure 2: Geological map of the Tapira Alkaline-Carbonatite Complex, showing the distribution of the studied boreholes. (Adapted from Brod et al., 2013).

Four probes were used to measure five geophysical parameters, including: density (gamma-gamma), the diameter of borehole (caliper) and the natural gamma, in addition to the acoustic and optical images. The gamma-gamma log was the main point of analysis in all boreholes and the caliper and natural gamma logs, as well as images from the televiewers were used in a complementary mode to visualize the walls of the borehole. All the acquired logs record cm by cm, thus providing a continuous record of rock parameters throughout the entire logged interval.

The density log was carried out with the HDGS (High Density Gamma Probe), which uses a radioactive source (^{137}Cs) at the bottom of the probe to bombard the borehole wall with gamma radiation. Some of these particles are reflected by geological material and captured by two sensors on the tool. This interaction of gamma radiation is known as Compton scattering (Almeida, 2011). This probe needs to be in contact with the rock to operate properly, so it has an arm that pushes it laterally and presses it against the borehole wall.

The HRD (High Resolution Density) sensor is located closer to the Caesium-137 source and is responsible for counting the radiation reflected laterally from the material closest to the tool, while the LSD (Long Spacing Density) sensor counts the radiation reflected from further distance. The relationship between counting and density is described by an exponential decay equation:

$$N = N_0 e^{-\mu \rho_e x} \quad (1)$$

where N is the count recorded by the sensor, N_0 is the radiation count emitted by the source, μ is the mass absorption coefficient, ρ_e is the electron density and x is the distance between the source and the sensor (Ellis and Singer, 2008). As the count is converted to electron density by the tool, this value is corrected to bulk density (ρ_{bulk}) using an equation that considers the atomic number (Z) and atomic mass (A) of the atoms that make up the geological material (Webber, 2008).

$$\rho_e = 2 \cdot \rho_{bulk} \cdot \frac{Z}{A} \quad (2)$$

Most geological materials exhibit a Z/A ratio close to 0.5, which implies $\rho_e = \rho_{bulk}$. However, elements like hydrogen, with Z/A ratio near 1, represent notable exceptions (Ellis and Singer, 2008). Thus, it remains appropriate to express ρ_e as defined in Equation 2.

The natural gamma log is performed by the same probe that is responsible for density measurement. The scintillometer embedded in the probe detects the natural radiation of the rock, which is produced by the decay of the Uranium group (^{235}U and ^{238}U), Thorium (^{233}Th), and Potassium (^{40}K) (Bateman, 2015).

The three-arm caliper (3-Arm Caliper Probe – 3ACS) is a probe that records the variation of the internal diameter along the borehole. The log generated by this probe allows integrity of the borehole to be assessed and identifies potential problems such as caves or tight spots that may interfere with other data.

One optical televiewer (OTV) and one acoustic televiewer (ATV) were used in some of the boreholes investigated, both of which generate a 360° image of the borehole wall. The High Resolution Optical Televiewer (Hi-OTV) generates the real image of the borehole using a camera. The High Resolution Acoustic Televiewer (HiRAT), on the other hand, generates the image from the amplitude of the acoustic pulses emitted by the probe and reflected off the borehole wall, with image acquisition dependent on probe being immersed in a liquid medium. Both televiewers require the support of centering devices to remain stable in the center of the borehole and to capture the image appropriately (Williams and Johnson, 2004).

During the data acquisition, core descriptions and the definition of the geological intervals were conducted in parallel by geologists of the same team for the boreholes investigated through well logging. These descriptions delineated the weathering horizons for each borehole considering textural aspects, color variation, and the integrity of the samples.

The traditional hydrostatic balance method is currently employed at the Tapira Mining Complex to obtain density values of core samples based on Archimedes' Principle, by measuring their mass both outside and inside water and relating it with the displaced water volume to find the density of the samples (Lipton, 2001). The core samples used in the density tests are on average 14 cm in length and 67.4 mm in diameter. The samples are routinely selected based on color, texture and mineralogical variations throughout the core and are packed in PVC bags before testing.

Eighty-five samples were selected for density determination through laboratory testing, representing the total number of samples from all the boreholes addressed in this study. These samples were selected based on the geological descriptions. Out of these, ten samples were excluded as they did not meet the proper conditions for the application of the hydrostatic balance method. However, this study considered only sixty-eight samples to ensure that the analysis intervals were similar to those of the logs.

The data obtained from well logging were interpreted and correlated with each other, considering the variations of the logs, the lithological intervals, and the previously described weathering horizons. In addition, the density logs were compared to the measurements obtained from the recovered core sample tests conducted in the laboratory to analyze the difference between the results produced by different methods in the same boreholes.

RESULTS

The logs generated during the data acquisition campaign totalized 1,351.07 m, encompassing caliper, density, natural gamma, and acoustic and optical televiewers measurements. Of this total, the caliper accounted for 379.90 m (28.1%), density for 370.59 m (27.4%), and natural gamma for 365.59 m (27.1%). Additionally, ATV contributed 83.35 m (6.2%) and OTV 153.18 m (11.3%) of the data acquired (Table 1).

Table 1: Data logging length and physical properties per borehole during the acquisition campaign.

| Boreholes | Caliper (m) | Density (m) | N. Gamma (m) | ATV (m) | OTV (m) |
|------------------------------|---------------|---------------|---------------|--------------|---------------|
| DH-1398 | 100.03 | 99.12 | 98.12 | | 48.03 |
| DH-1399 | 49.93 | 49.12 | 48.12 | 46.29 | |
| DH-1400 | 122.97 | 122.23 | 121.23 | | 33.00 |
| DH-1402 | 57.93 | 52.00 | 51.00 | | 53.93 |
| DH-1403 | 49.04 | 48.12 | 47.12 | 37.06 | 18.22 |
| TOTAL ACQUISITION (m) | 379.90 | 370.59 | 365.59 | 83.35 | 153.18 |

The DH-1400 borehole presented the deepest logging measurements, with data exceeding 120 m in depth, followed by DH-1398, DH-1402, and DH-1399. The borehole with the shallowest logging extent was DH-1403, which reached less than 51 m in depth (Figure 3).

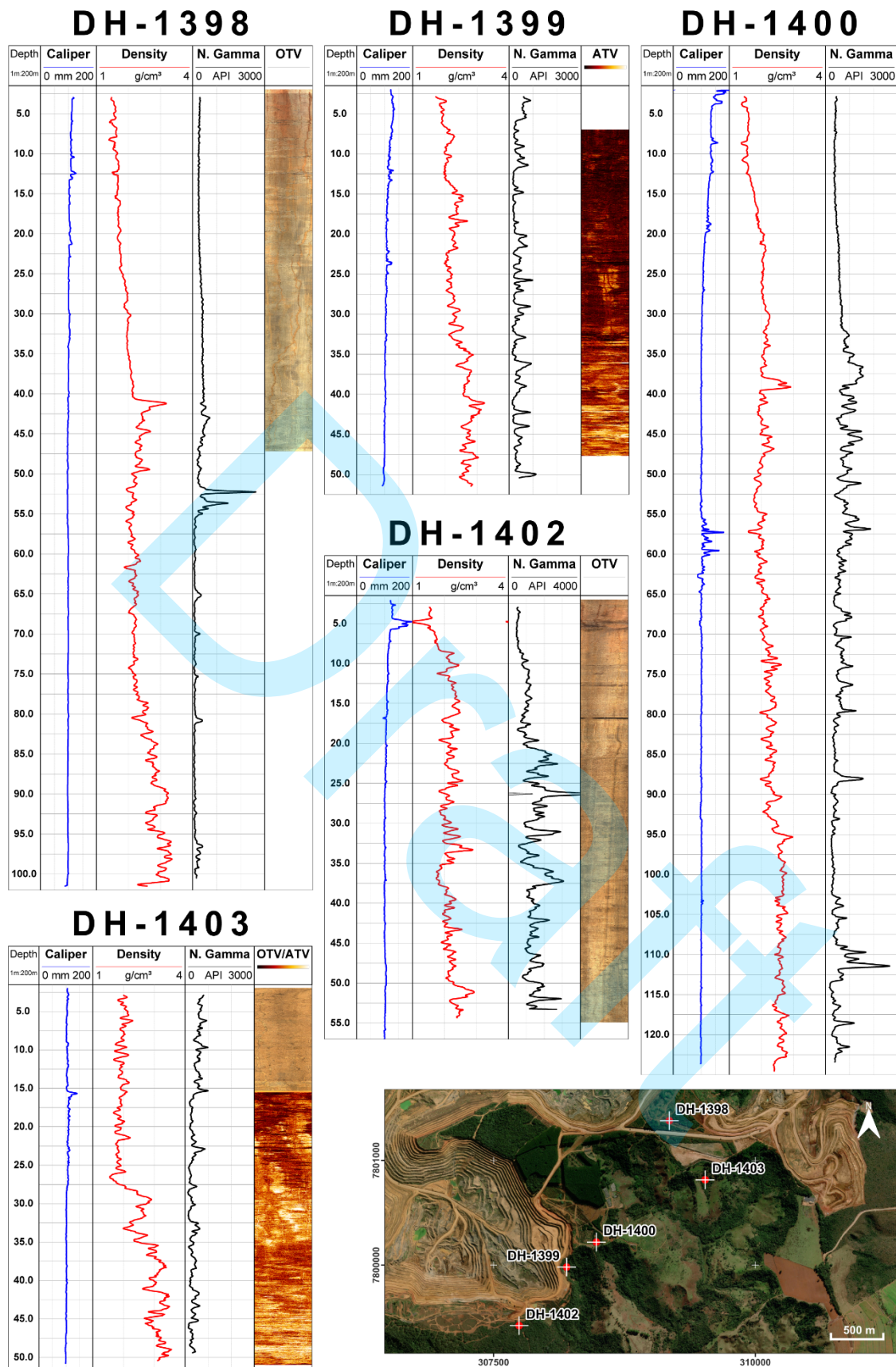


Figure 3: Logs from each borehole, including caliper, density, natural gamma, and optical / acoustic image data, and their spatial distribution.

Bulk density

The density logs, which were the primary focus of the data acquisition campaign, reveal a systematic trend across the five boreholes, particularly in the deeper sections. At shallower depths, density values typically remain below 2 g/cm^3 , with an average of approximately 1.6 g/cm^3 . An exception occurs in the DH-1403 log, where the recorded density averages 2 g/cm^3 .

This upper section is characterized by relatively consistent readings with a gradual increase in density with depth, occasionally interrupted by minor low-density peaks. A second interval begins with an abrupt change from the upper pattern. In this region, the gamma-gamma logs become more irregular, featuring numerous small peaks and at least one significant peak reaching the highest density within this range. Densities slightly exceed 2 g/cm^3 , averaging between 2.1 and 2.2 g/cm^3 , with maximum values approaching 3 g/cm^3 . Within this interval, the highest density values are typically located near its top and base, while the central portion exhibits lower densities, forming a concave trend.

The third interval, corresponding to the basal sections of the boreholes, is marked by another abrupt change in behavior. This region contains the highest density measurements, often approaching or exceeding 3 g/cm^3 , particularly in DH-1398 and DH-1403. In this interval, the logs become highly irregular, with pronounced positive and negative excursions and an overall trend of increasing density towards the base of the log. An exception is observed in DH-1400, where the basal interval is more consistent and regular of higher values. Additionally, this interval is notably thinner in DH-1402 compared to the other boreholes.

Caliper

The caliper logs display a clear trend where deeper sections exhibit less variation in diameter. In these deeper zones, occurrences of breakouts or constrictions—indicated by sudden diameter changes—are not common. The logs predominantly show a stable diameter near 100 mm, slightly larger (by approximately 4 mm) than the drilled diameter. However, borehole DH-1400 deviates from this trend between the interval 55 and 65 m, where the caliper log indicates significant fluctuations, peaking over 180 mm.

In the upper sections, the caliper logs are more irregular, with frequent abrupt diameter increases. A characteristic "funnel-like" shape is evident near the surface, extending to depths of 20–30 m. This feature is most pronounced in borehole DH-1400 and less prominent in DH-1403.

Among the boreholes, DH-1400 shows the largest positive and negative variations in diameter. In contrast, DH-1398 and DH-1402 maintain a more stable caliper log, even at shallower depths. Despite these variations, the overall caliper behavior is consistent across the five boreholes, reinforcing the reliability of the caliper log for interpreting other physical parameters, particularly density, which is closely tied to the caliper data.

Natural gamma

The natural gamma logs exhibit significant variability, making it challenging to establish consistent patterns throughout the boreholes. Boreholes DH-1398 and DH-1400 show comparable behavior in their upper sections, recording radiation levels ranging from 230 to 470 API in DH-1398 and 350 to 700 API in DH-1400. Both logs display minimal variation and a slight increase in values at 41 m in DH-1398 and 31 m of depth in DH-1400. Below these depths, significant variations emerge, reducing the correlation between the two logs.

In the deeper intervals, radiation levels generally decrease. In DH-1398, values drop below 100 API, with the log becoming nearly uniform below 55 m. Conversely, DH-1400 exhibits alternating high and low values throughout its deeper sections. Both logs feature prominent radiation peaks, exceeding 2600 API at 52 m in DH-1398 and 111 m in DH-1400.

The natural gamma log for DH-1402 displays similar upper-interval behavior but with considerably higher radiation levels, exceeding 1000 API. Its maximum peak, exceeding 5300 API, occurs at a depth of 26 m, closer to the surface, similar to DH-1398. In the deeper sections, the log alternates between high and low radiation levels, maintaining significant variability. Overall, DH-1402 presents the highest readings among the five analyzed boreholes.

The logs from boreholes DH-1399 and DH-1403, corresponding to shallower intervals, lack well-defined patterns. They maintain average values of approximately 360 API and 400 API, respectively, with radiation peaks interspersed throughout. Both logs record maximum values around 1000 API, indicating less variability compared to the deeper boreholes.

Televewers

Optical images were acquired for boreholes DH-1398, DH-1402, and DH-1403, while acoustic images were obtained from DH-1399 and DH-1403. The imaging tools provided limited data compared to other logs due to technical constraints. The acoustic televiewer (ATV) requires immersion in fluid to operate, while the optical televiewer (OTV) needs good conditions of visibility, which was impaired by the high turbidity of the borehole fluid. To enhance data interpretation for borehole DH-1403, a composite log combining both image types was created.

The imaging tools corroborated caliper log findings by highlighting areas of increased borehole diameter. The OTV, which captures the borehole wall's texture and roughness, corroborated these features. However, the optical images did not provide enough detail to define the boundaries of the weathered profile or to identify well-defined structures such as fractures, faults, cementation coefficient clearly.

The ATV, in contrast, produced images that also captured wall roughness and data amplitude variations, with color contrast indicating transit time variations due to the rock matrix and fluids. These images revealed a gradual tonal shift, transitioning from darker to lighter shades toward the borehole bottoms. In DH-1399, this gradation was interrupted by a sudden tonal change at 41.3 m of depth. Additionally, the ATV identified structures or textures represented as sinusoidal

patterns, which were more frequently observed at greater depths, providing valuable insight into subsurface conditions.

Core samples

The geological description defined the weathering horizons for each borehole and classified the parent rock as bebedourite for all boreholes. Subsequently, core samples were selected from several depths in each borehole for density testing. The sampling range defined in this study encompassed all weathering horizons in boreholes DH-1398 and DH-1400, including aloterite, isalterite, saprolite, and fresh rock. Borehole DH-1399 comprised samples of isalterite, saprolite and fresh rock, but no aloterite was collected. Borehole DH-1402 reached only aloterite and isalterite samples, whereas DH-1403 provided samples of isalterite and fresh rock.

The laboratory density measurements obtained indicate a regular increase in density with depth (Table 2). The average density for the aloterite was 1.44 g/cm³; for the isalterite, it was 1.72 g/cm³; and the saprolite recorded an average density of 2.01 g/cm³, while fresh rock exhibited an average density of 2.58 g/cm³. Only four samples displayed densities higher than 3 g/cm³, all of which were selected from the fresh rock. Some samples exhibit low values at deeper points, such as the sample at 58.63 m, which shows a density of 1.07 g/cm³.

Table 2: Laboratory bulk density measurements of core samples, positioned within their respective weathering horizons as defined by the geological description.

| DH-1398 | | | DH-1399 | | | DH-1400 | | | DH-1402 | | | DH-1403 | | |
|-----------|-----------------------------------|------------|-----------|-----------------------------------|------------|-----------|-----------------------------------|------------|-----------|-----------------------------------|-----------|-----------|-----------------------------------|------------|
| Depth (m) | Bulk density (g/cm ³) | Horizon | Depth (m) | Bulk density (g/cm ³) | Horizon | Depth (m) | Bulk density (g/cm ³) | Horizon | Depth (m) | Bulk density (g/cm ³) | Horizon | Depth (m) | Bulk density (g/cm ³) | Horizon |
| 3.5 | 1.27 | Aloterite | 4.75 | 1.56 | Isalterite | 0.31 | 1.16 | Aloterite | 0.48 | 1.4 | Isalt. | 8.26 | 1.88 | Isalterite |
| 12.1 | 1.26 | | 9.24 | 1.7 | | 8.13 | 1.25 | | 3.54 | 1.56 | | 11.17 | 1.89 | |
| 13.3 | 1.27 | | 24.23 | 1.78 | | 12.68 | 1.23 | | 18.81 | 2.12 | | 14.62 | 1.65 | |
| 23.2 | 1.33 | | 28.5 | 1.89 | | 19.19 | 1.42 | | 29.8 | 1.86 | | 16.73 | 1.71 | |
| 26.7 | 1.5 | | 37.27 | 2.27 | | 24.1 | 1.45 | | 40.94 | 1.9 | | 18.91 | 1.67 | |
| 32 | 1.52 | Isalterite | 39.33 | 1.94 | Saprolite | 29.78 | 1.57 | Isalterite | 49.58 | 2.33 | Saprolite | 22.29 | 1.55 | Fresh rock |
| 37.6 | 1.63 | | 43.12 | 1.78 | | 33.67 | 1.46 | | | | | 26.05 | 1.5 | |
| 42.6 | 1.89 | | 48.68 | 1.83 | | 37.27 | 1.26 | | | | | 28.22 | 1.17 | |
| 47.3 | 1.64 | | 51.71 | 3.51 | | 39.18 | 1.55 | | | | | 30.53 | 2.04 | |
| 52.4 | 1.36 | | 52.67 | 2.38 | | 47.95 | 1.29 | | | | | 33.53 | 2.25 | |
| 60.1 | 1.68 | Fresh rock | 54.83 | 1.9 | FR | 58.63 | 1.07 | Saprolite | | | | 35.65 | 2.1 | |
| 65.7 | 2.45 | | | | | 78.15 | 1.68 | | | | | 48.35 | 2.58 | Fresh rock |
| 74.2 | 1.55 | | | | | 84.88 | 1.79 | | | | | 49.42 | 2.87 | |
| 97.6 | 1.46 | Saprolite | | | | 92.13 | 1.59 | | | | | 50.28 | 3.03 | |
| 99.3 | 2.65 | | | | | 98.93 | 1.84 | | | | | | | |
| 99.8 | 2.74 | | | | | 111.58 | 2.3 | | | | | | | |
| 102.8 | 3.08 | | | | | 121.35 | 2.75 | | | | | | | |
| 103.5 | 2.63 | | | | | 127.68 | 1.99 | | | | | | | |

INTERPRETATION OF WELL LOG DATA

The caliper logs exhibit consistent diameter measurements, indicating no expressive alterations in the borehole walls. However, a gradual widening toward the surface is evident, likely caused by the final stages of drilling, where the removal of casing rods enlarges the borehole's upper

section. Positive diameter peaks reflect wall breakouts, which compromise borehole integrity and interfere with logs like density. Negative peaks, less frequent and occurring only in DH-1400 and DH-1402, indicate constrictions. These anomalies, with variations ranging from 7% to 18%, are concentrated in the upper regions, usually corresponding to the aloterite, due to the more unconsolidated material of the weathering mantle. In contrast, deeper sections, consisting of less weathered rock (saprolite and fresh rock), exhibit better geological stability (Figure 4).

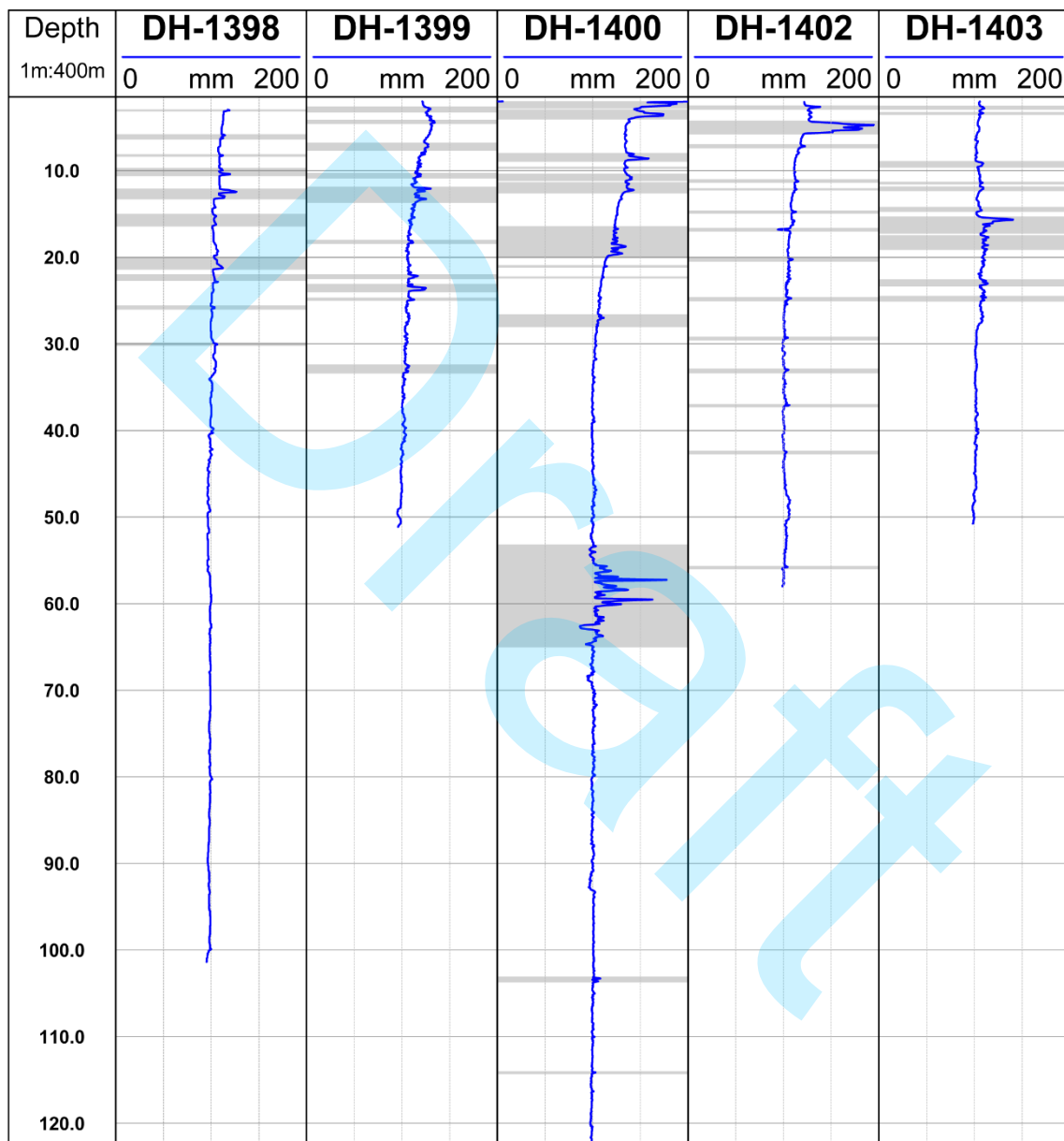


Figure 4: Caliper logs. The gray bands indicate zones where the borehole walls exhibited alterations. Positives shifts indicate breakouts and negatives express wall constrictions.

Natural gamma logs reveal significant variability, which is typical of areas characterized by high geological complexity such as areas formed by igneous intrusions. Positive radioactivity peaks are related to zones with mineral accumulations containing isotopes of U, Th, and K. Comparison between gamma and density logs, particularly in DH-1398, DH-1400, and DH-1402,

suggests a correlation surface marked by abrupt changes at the transition between upper and intermediate horizons (Figure 5). These characteristics are similar to the geochemical analyses of radionuclides conducted by Conceição and Bonotto (2006) on samples taken from all weathering horizons as well as fresh rock.

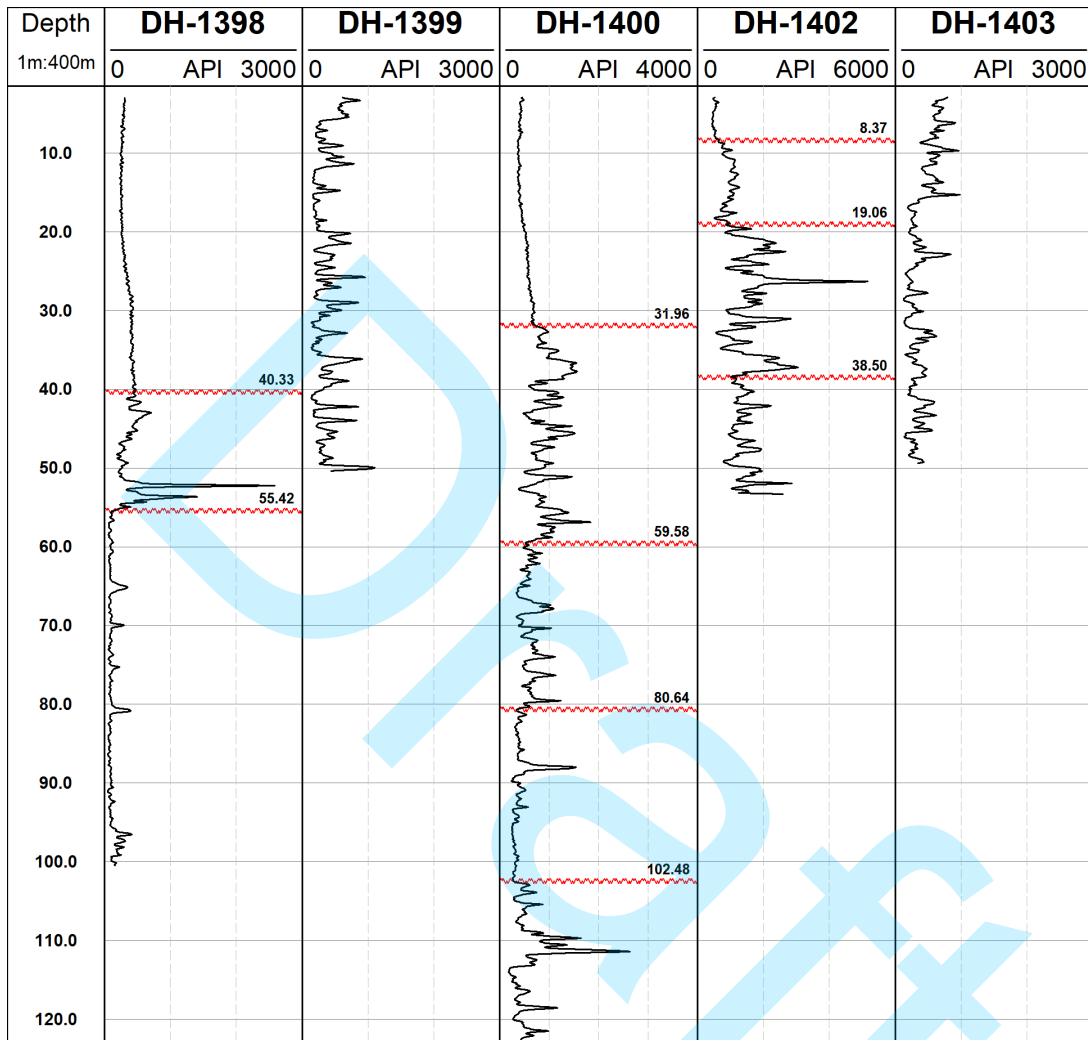


Figure 5: Natural gamma logs. The main shifts in trends are indicated by horizontal red lines.

The density logs delineate three main zones based on weathering horizons. The uppermost zone, the aloterite, with densities around 1.5 g/cm^3 , reflecting highly porous and weathered zone characterized by lighter element concentration. The intermediate zone, the isalterite, with densities around 2.2 g/cm^3 as a result of less altered and with denser element concentration. This zone hosts secondary phosphate mineralization and is the target of mining activities. At greater depths, the logs record densities between 2.6 and 3.2 g/cm^3 , characteristic of fresh or minimally altered rock, with low porosity and preserved protolith features (Figure 6).

Negative density peaks, prevalent in the aloterite, usually correspond to positive caliper peaks. These occur because density tool sensors lose contact with the rock during wall breakouts, causing abrupt drops in readings. These intervals require attention during density log analysis to avoid interference with the interpretation.

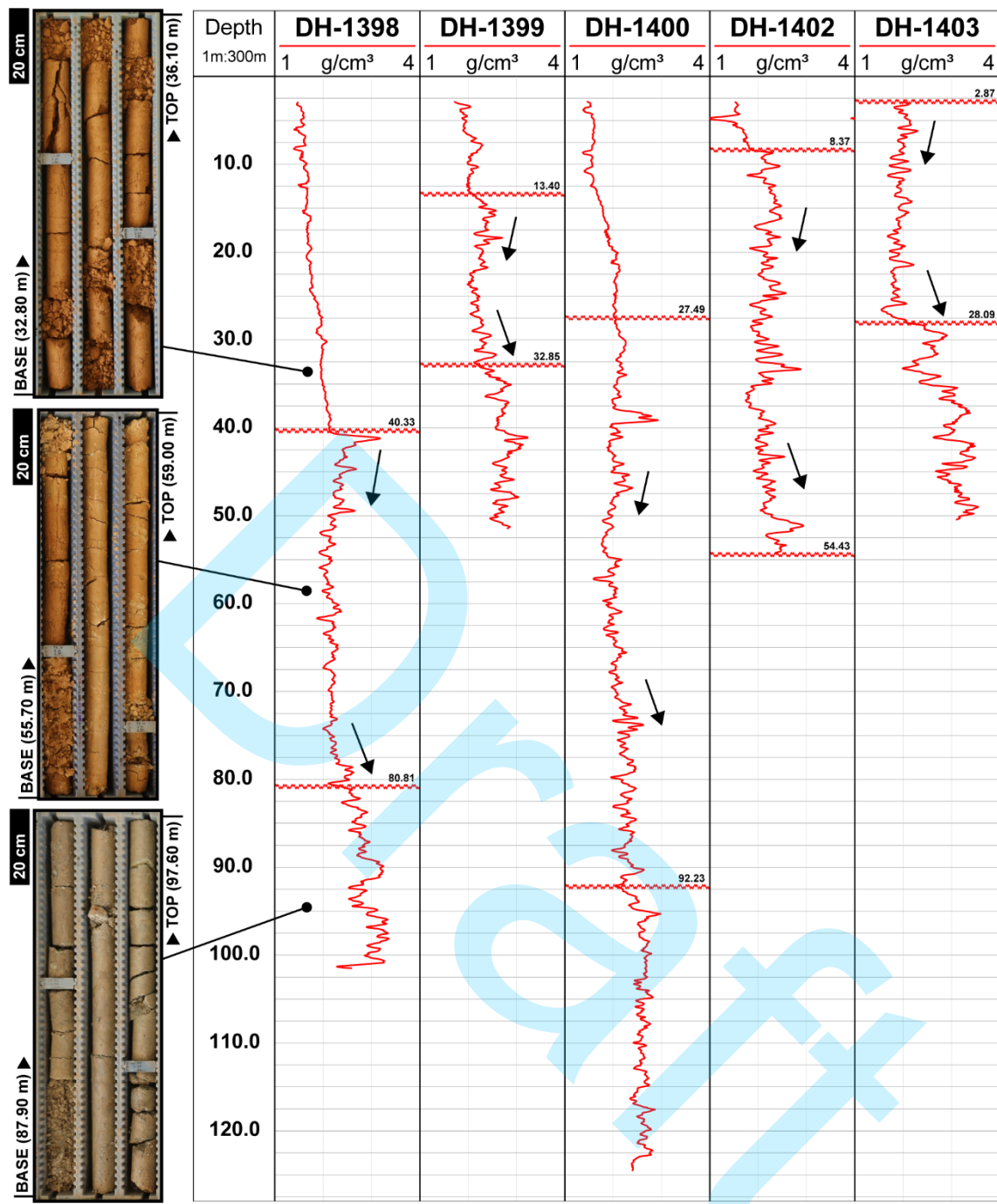


Figure 6: Density logs with their compartmentalization highlighted and exemplified by core samples. The arrows indicate the trend of the lines within the phosphate mineralized interval.

The images generated by the OTV highlighted the visual homogeneity of the rock, which is linked to the weathering process, especially at shallower depths where the images could be captured. In contrast, the ATV images revealed how the rock becomes progressively less affected by weathering with increasing depth. Lighter tones correspond to less altered rocks, where acoustic waves return more easily. This characteristic becomes more pronounced in the images as the depth increases (Figure 7). The vertical features in the images are attributed to marks left by the caliper arms operated prior to the televiewer survey.

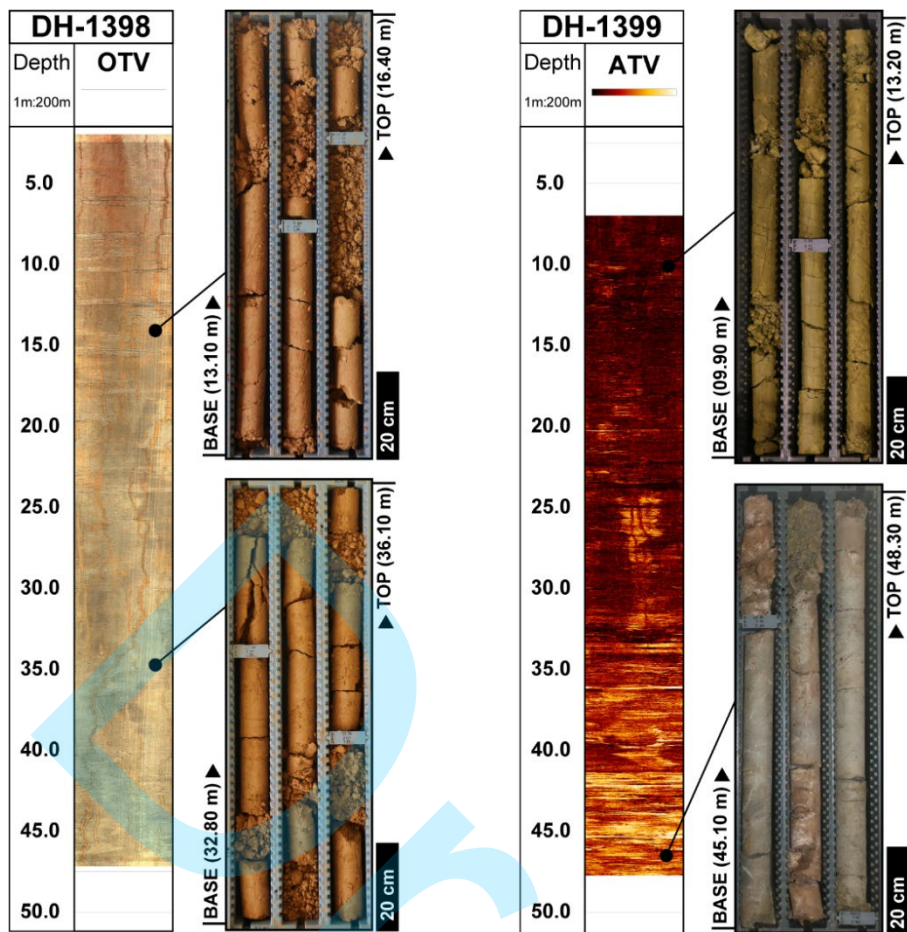


Figure 7: Image logs of boreholes DH-1398 and DH-1399 compared to the drill core samples. Homogeneity is observed in the OTV of DH-1398, while the variation in weathering intensity is evident in the ATV of DH-1399.

DISCUSSION

Delineation and correlation of the phosphate zone

The boundaries established from the core descriptions were correlated with the gamma-gamma logs aiming to identify the isalterite (the phosphate mineralized horizon) using geophysical data and considering the three common intervals observed in the acquired logs. In this context, it was observed that there was predominantly no exact match between the two methods for establishing the mineralized interval, with discrepancies reaching up to 20 m in the position of the horizon boundaries.

The well logging approach helps to reduce subjectivity, as it focuses solely on the analysis of numerical values expressed in the logs, which present trends and variations directly linked to the rock's characteristics such as mineralogical assemblage, density and porosity. As seen in the images generated by the OTV, the homogeneity of the core samples can hinder the boundaries between weathering horizons, possibly leading to misinterpretations and potentially reducing the thickness of the main horizon of exploration.

Based on this, it is proposed that the isalterite corresponds to the intermediate interval

observed in the geophysical logging acquisitions (Figure 8). Within this horizon, density measurements typically range between 1.9 and 2.2 g/cm³, displaying a normal distribution. Positive and negative anomalous values are associated with concentrations of heavier minerals (such as magnetite) or with silicified intervals, respectively.

The natural gamma logs are also useful for this determination, as the accumulation of radionuclides described by Conceição and Bonotto (2006) coincides with the boundary between the aloterite and isalterite horizons. High values in the natural gamma logs can thus be correlated with the characteristic pattern shifts observed in the density logs. In boreholes where the weathering mantle is more developed, the natural gamma log in the aloterite tends to show lower and less variable readings. This characteristic is associated with the intense leaching process to which the horizon has been subjected. This process removes micaceous minerals from the aloterite, directly influencing natural radiation readings.

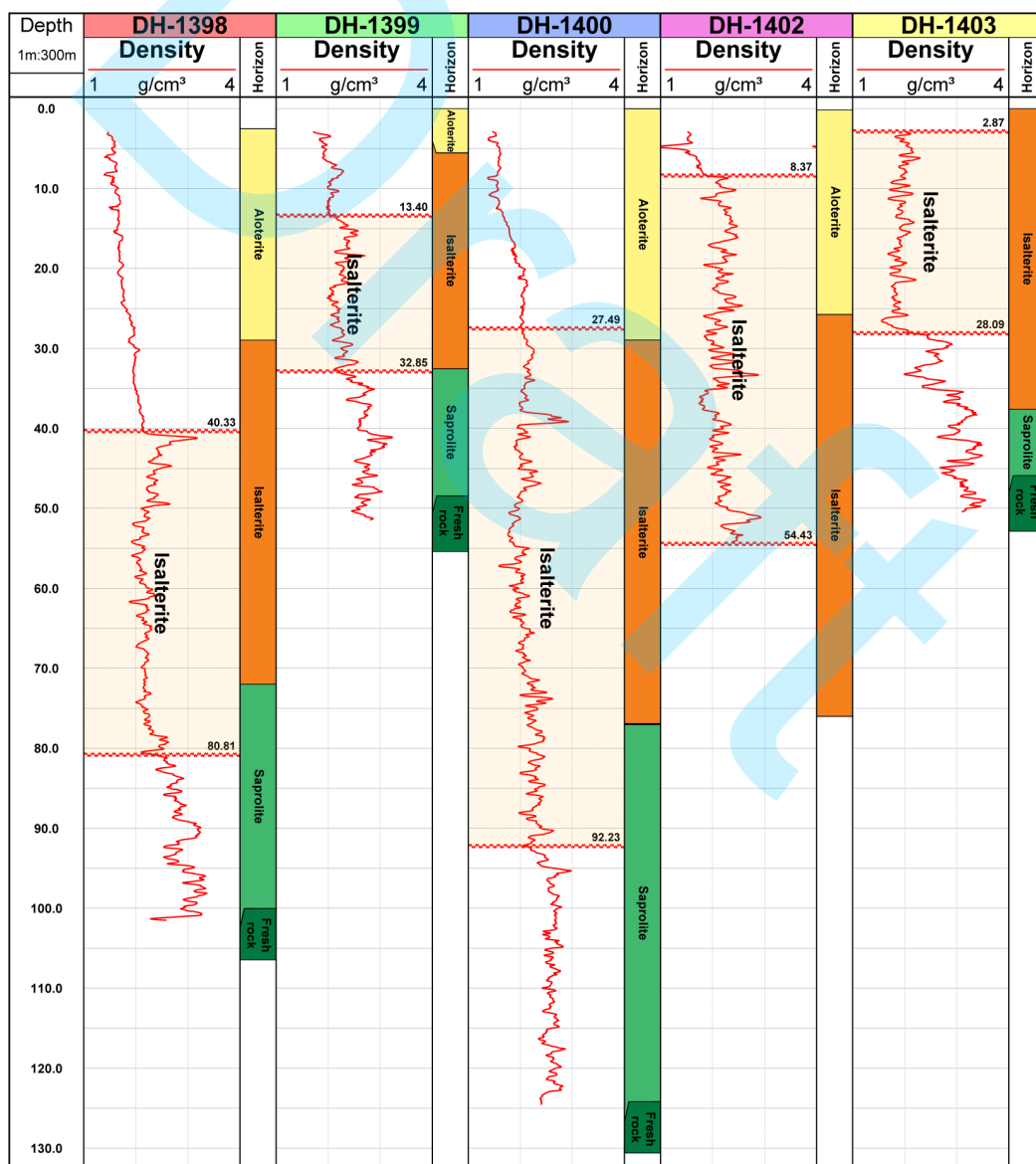


Figure 8: Delimitation of the isalterite based on density logs compared with boundaries defined by traditional geological description.

In a comparative analysis between the natural gamma and density logs in borehole DH-1398, it is observed that the aloterite is less dense and less radioactive. In contrast, starting from the isalterite, the density and the natural gamma increase and show significant variation, marking the boundary between the horizons at 40.33 m. However, the beginning of the isalterite is not explicitly apparent in a visual analysis of the core, considering both the geophysically determined boundary and the one established through geological description at 29 m (Figure 9). In this case, the geological description considers 11 m of geological material as mineable; however, this interval does not exhibit physical characteristics consistent with the isalterite as determined by geophysical logging.

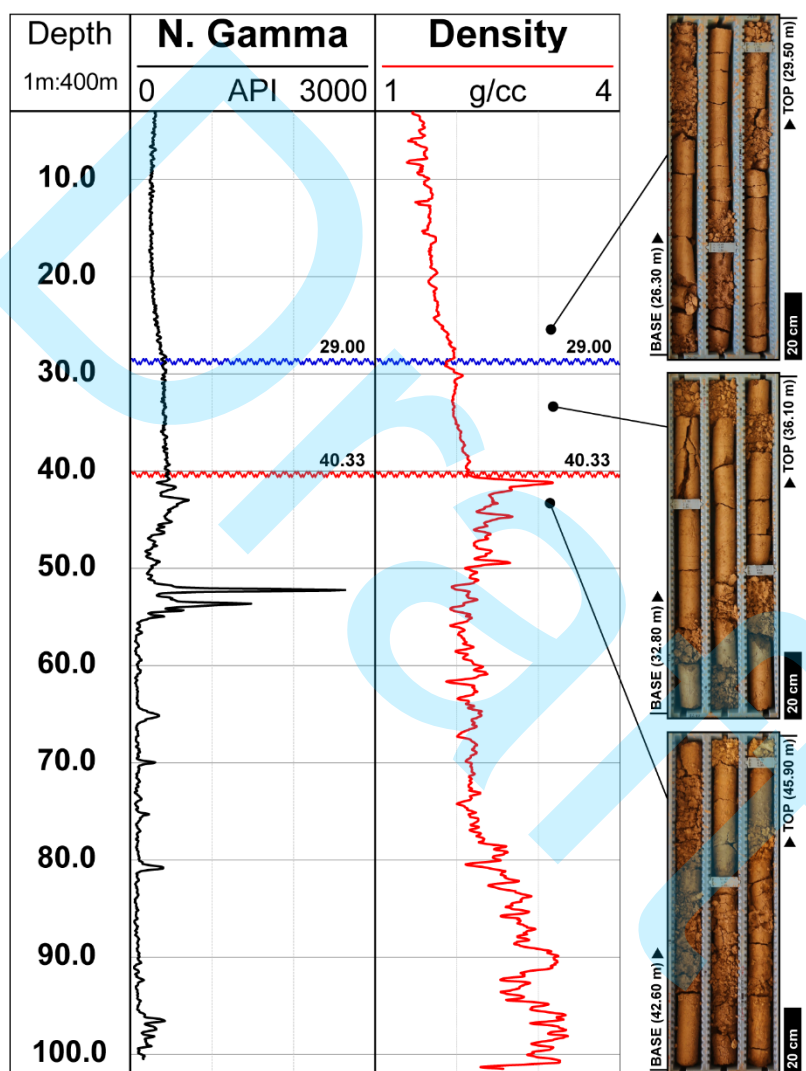


Figure 9: Natural gamma and density logs indicating the boundary between aloterite and isalterite in the borehole DH-1398. The blue horizontal line represents the boundary defined by the geological description, while the red horizontal line marks the division based on the correlation of the logs.

With these data integrated into the analysis of density measurements across all logs, a correlation was established between the logs to delineate the mineralized interval (Figure 10). This study does not include detailed geological-structural mapping; therefore, the proposed correlation is based only on the variation in thickness of the interval of interest and its spatial distribution across the TMC.

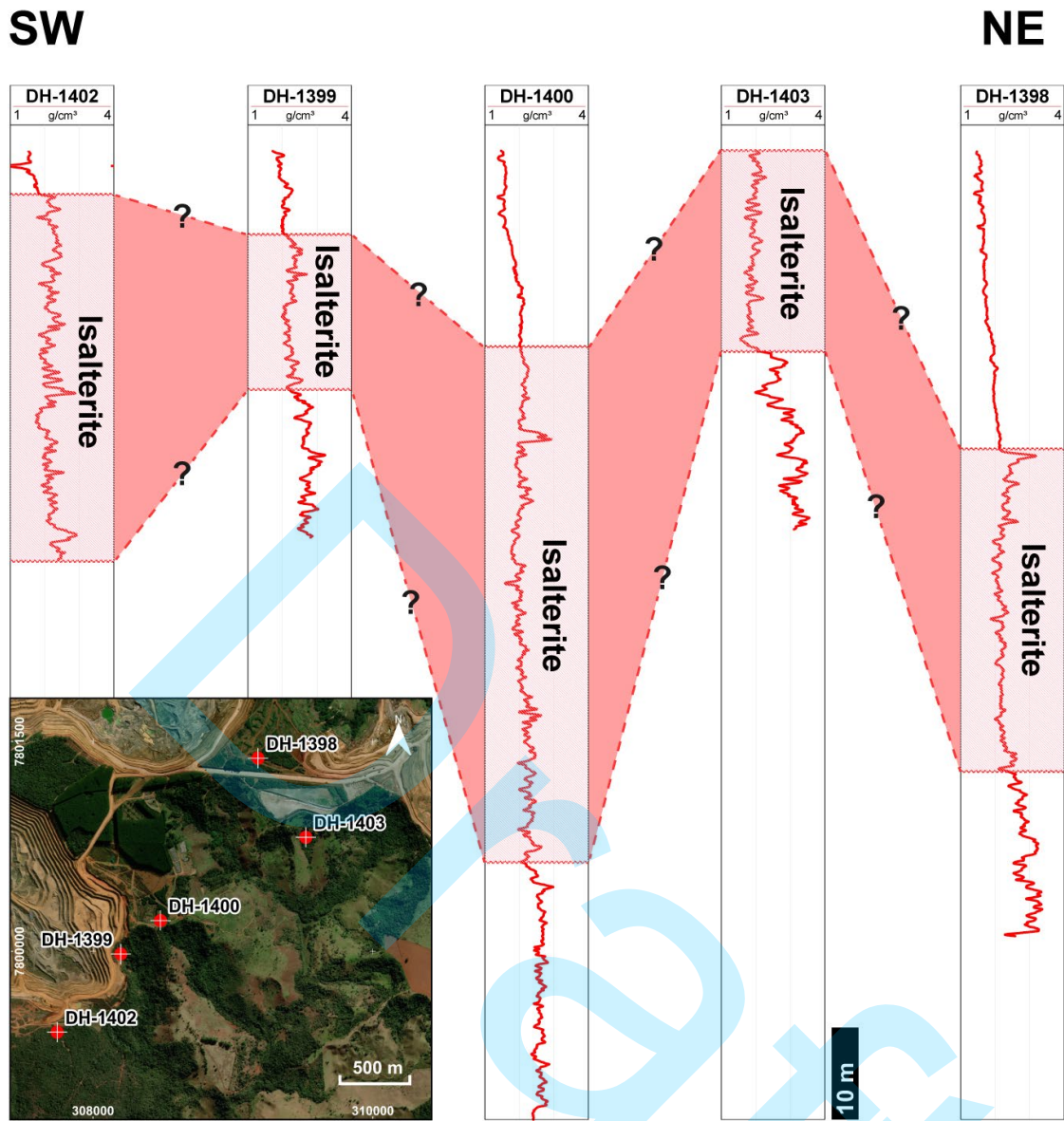


Figure 10: Correlation of the isalterite horizon based on interpretation of well logs following a SW-NE section across the Tapira Mining Complex.

Well logging data compared to Laboratory measurements

In addition to the lithological description, the geological material underwent density measurements using the hydrostatic weighting method (Lipton and Horton, 2014). When comparing the data obtained from well logging with the traditional methodology, it was observed that the measurements from the geophysical method were predominantly higher, with differences exceeding 1 g/cm^3 . This difference can be observed across all horizons; however, DH-1402 is an exception, as the average trend of the density logs and laboratory measurements are almost the same (Figure 11).

The most notable region is in the lower part of DH-1398, an interval where weathering is less intense and shows the greatest difference among all the investigated boreholes. This notable discrepancy is primarily attributed to factors such as the integrity of the core samples and the subjectivity inherent to the laboratory methodology.

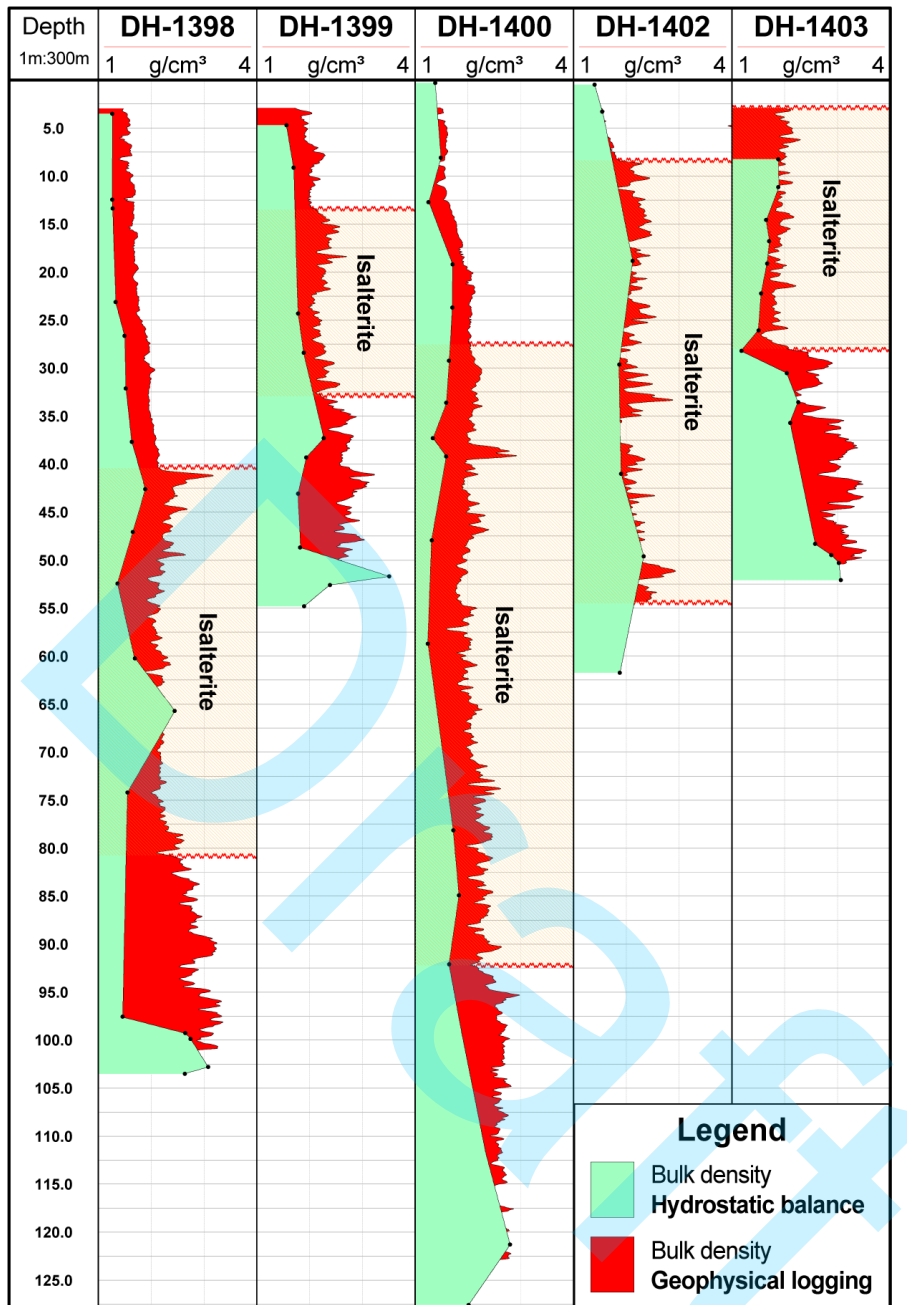


Figure 11: Comparison of density estimates derived from the hydrostatic method and geophysical logging. The estimates obtained using the traditional method were interpolated and presented as logs.

As the analyzed material is part of a weathering mantle, the core samples obtained through drilling are predominantly unconsolidated or intact due to a cementation process, which directly impacts laboratory analysis (Figure 12). During the testing process, the samples must be enclosed in plastic material, which also traps air along with the solid material. This inclusion of air affects the sample's density, causing the values to decrease. Another case of interference occurs when the samples selected for analysis are from an interval of intense cementation. This process, commonly associated with silica, helps preserve the integrity of the samples; however, it skews the density measurements.



Figure 12: Unconsolidated sample cores characteristic of aloterite and isalterite. The image represents the interval 29 - 39 m of the borehole DH-1400.

The fact that well logging is an in-situ application implies that measurements are taken under natural moisture conditions and higher confining pressure compared to tests conducted on core samples. At greater depths, rocks are subjected to increased loads due to the overlying geological material. As a result, their volume may decrease, leading to an increase in density. Regarding moisture, samples tend to lose water in their way from removal of the drill hole and the density test, especially those rich in clays and clay minerals that have fissures. Consequently, these samples are not under confining pressure and are typically less moist than the rock in its natural state.

In addition to the preservation state of the samples, subjectivity also contributes to data alteration, as the geologist selecting the samples for analyses often tends to choose the most intact ones. However, the integrity of such samples can be associated with the presence of more competent material that has been less affected by weathering processes. The influence of the individual conducting the laboratory analysis is also evident in the results from samples obtained at greater depths, which are consequently more intact due to reduced weathering effects. These cases highlight that this type of approach is more susceptible to errors associated with human bias, further compromising the reliability of the data.

Thus, both factors reduce the reliability of laboratory-obtained density data, as they are highly susceptible to external influences. Notably, there is an inconsistency in the density values

for upper portions, which sometimes approach to 1 g/cm³ (the density of water), as well as a marked difference in deeper horizons between the two methodologies. Geophysical logging, using the probe properly calibrated, shows that density measurements are more reliable considering the nature, state and composition of the geological material.

The data acquisition time and resolution are also important in this comparison. Density logging is conducted at an average speed of 4 m/min, meaning that logging a 100-meter borehole can only take approximately 25 to 30 min to be fully performed. This efficiency allows data to be acquired for 2 or 3 boreholes in a single workday, factoring in the time required for equipment setup, in contrast to laboratory measurements which require about a week to analyze a whole core. In addition to the time, wireline well logging provides measurements at every centimeter of rock, which is a stark contrast to laboratory measurements, typically taken at irregular intervals ranging from 1 to 15 m between sampling points, resulting in a core with considerable gaps between the selected samples. The deepest borehole in this study, the DH-1400, for example, displays 21 density tests, contrasting with more than 12,000 geophysical readings.

CONCLUSIONS

Bulk density is crucial data for mineral exploration, and when this information is provided reliably and with minimal interference, it becomes even more valuable for mining companies. Based on the density measurements obtained through well logging in the five investigated boreholes, the method showed excellent performance in determining the physical property of the phosphate-rich rocks of the Tapira Alkaline-Carbonatite Complex.

Compared to the traditional method based on Archimedes' principle, the geophysical logging results provided higher-resolution measurements that were predominantly superior and more consistent. Since sampling is hindered by the condition of the drill cores and subjective factors in sample choice and preparation, the hydrostatic balance method struggles more to eliminate external influences in the data and requires more time to achieve results. In addition, the acquisition of geophysical data occurs in-situ and in a significantly shorter time, with the possibility of being monitored in real-time during the data collection process.

The gamma-gamma density logs also enabled the delineation of the interval where mining operations occur at the TMC, highlighted by a range of 1.9 - 2.2 g/cm³, which had considerable differences in both the thickness and depths of its boundaries compared to the geological description. In contrast to an empirical methodology of observing drill cores, the geophysical method proposes this delineation based on physical rock properties, such as density and natural radiation. With higher resolution, greater data reliability, and reduced subjectivity, the understanding of the compartmentalization of the weathering profile in the alkaline-carbonatite complex becomes even clearer. Thus, density data obtained through geophysical logging, complemented by other physical and chemical properties of the rocks, can serve as a powerful

alternative for both mineral resource estimation and mine planning, while also contributing to optimization in the exploration process.

ACKNOWLEDGEMENTS

The authors thank Mosaic Fertilizantes do Brasil for the financial support through the R&D project, Desenvolvimento de Perfilagem Geofísica de Poços em Rochas do Complexo Carbonatítico da Mosaic Fertilizantes (IGEO 23.455). We would also like to thank the Technician José Roberto Delboni and Wanderlei de Sousa for his support in data acquisition. We would also thank Kyle Owen (Robertson Geologging) for their assistance with technical issues with the logging tools.

REFERENCES

ANM, Agência Nacional de Mineração. 2019. Sumário Mineral 2018 [Annual Mineral Survey 2018]. Brasília, Brazil: ANM.

Abram, M. B., I. C. Bahiense, C. G. Porto, and R. S. C. Brito. 2011. Projeto Fosfato Brasil – Parte I. Informe de Recursos Minerais. Série Insumos Minerais para Agricultura, no. 13. Salvador, Brazil: CPRM. <https://rigeo.sgb.gov.br/handle/doc/14807>.

Abram, M. B., I. A. Cunha, and R. C. Almeida. 2016. Projeto Fosfato Brasil – Parte II. Informe de Recursos Minerais. Série Insumos Minerais para Agricultura, no. 17. Salvador, Brazil: CPRM. <https://rigeo.sgb.gov.br/handle/doc/16142>.

Almeida, T. 2011. A perfilagem geofísica gama-gama em depósitos de ferro do Quadrilátero Ferrífero. Master's thesis, Universidade Federal do Rio Grande do Sul, Porto Alegre, Brazil. 181 pp. <https://lume.ufrgs.br/handle/10183/37384>.

Asfahani, J. 2002. Phosphate Prospecting Using Natural Gamma Ray Well Logging in the Khneifiss Mine, Syria. *Exploration and Mining Geology* 11 (1–4): 61–68. <https://doi.org/10.2113/11.1-4.61>.

Asfahani, J. 2019. Heat Production Estimation by Using Natural Gamma-Ray Well-Logging Technique in Phosphatic Khneifis Deposit in Syria. *Applied Radiation and Isotopes* 145 (March):209–16. <https://doi.org/10.1016/j.apradiso.2018.11.017>.

Asfahani, J., and A. Abdul-Hadi. 2001. Geophysical Natural γ -Ray Well Logging and Spectrometric Signatures of South AL-Abter Phosphatic Deposits in Syria. *Applied Radiation and Isotopes* 54 (3): 543–57. [https://doi.org/10.1016/S0969-8043\(00\)00290-6](https://doi.org/10.1016/S0969-8043(00)00290-6).

Barbosa, O., O. P. G. Braun, R. C. Dyer, and C. A. B. R. Cunha. 1970. Geologia da região do Triângulo Mineiro [Geology of the Triângulo Mineiro Region]. Boletim 136. Rio de Janeiro, Brazil: Departamento Nacional da Produção Mineral, Divisão de Fomento da Produção

Mineral, 140 pp.

Bateman, R. M. 2015. Cased-Hole Log Analysis and Reservoir Performance Monitoring. New York, NY: Springer. <https://doi.org/10.1007/978-1-4939-2068-6>.

Bezerra, M. A., and J. A. Brod. 2013. Mineralogia da Apatita do Complexo Alcalino-Carbonatítico de Tapira [Apatite Mineralogy of the Tapira Alkaline-Carbonatite Complex]. In Anais da 65^a Reunião Anual da Sociedade Brasileira para o Progresso da Ciência (SBPC), Recife, Pernambuco, Brazil, 14 pp.

Brasil. Secretaria Especial de Assuntos Estratégicos (SAE). 2021. Plano Nacional de Fertilizantes 2050 (PNF 2050): uma estratégia para os fertilizantes no Brasil. Brasília, Brazil. 195 pp.

Brasil. Secretaria Especial de Assuntos Estratégicos (SAE). 2023. Plano Nacional de Fertilizantes 2050 (PNF 2050): uma estratégia para os fertilizantes no Brasil. Brasília, Brazil. 197 pp.

Brod, J. A., C. C. Ribeiro, J. C. Gaspar, T. C. Junqueira-Brod, E. S. R. Barbosa, B. F. Riffel, J. F. Silva, N. Chaban, and A. J. D. Ferrari. 2004. Excursion 1: Geology and Mineralization of the Alkaline-Carbonatite Complexes of the Alto Paranaíba Igneous Province. In Proceedings of the 42nd Brazilian Geological Congress, Araxá, Minas Gerais, Brazil. 1–29.

Brod, J. A., T. C. Junqueira-Brod, J. C. Gaspar, I. A. Petrinovic, S. C. Valente, and A. Corval. 2013. Decoupling of Paired Elements, Crossover REE Patterns, and Mirrored Spider Diagrams: Fingerprinting Liquid Immiscibility in the Tapira Alkaline–Carbonatite Complex, SE Brazil. *Journal of South American Earth Sciences* 41 (January):41–56. <https://doi.org/10.1016/j.jsames.2012.04.013>.

Carasco, C., B. Pérot, J.-L. Ma, H. Toubon, and A. Dubille-Auchère. 2018. Improving Gross Count Gamma-Ray Logging in Uranium Mining with the NGRS Probe. *IEEE Transactions on Nuclear Science* 65 (3): 919–23. <https://doi.org/10.1109/TNS.2018.2800909>.

CIM, Canadian Institute of Mining, Metallurgy and Petroleum. 2018. CIM Mineral Exploration Best Practice Guidelines. Westmount, QC: CIM, 17 pp.

CIM, Canadian Institute of Mining, Metallurgy and Petroleum. 2019. CIM Estimation of Mineral Resources and Mineral Reserves Best Practice Guidelines. Westmount, QC: CIM, 75 pp.

Conceição, F. T., and D. M. Bonotto. 2006. Distribuição de Radionuclídeos, Metais Pesados e Flúor Em Perfis de Alteração Nos Complexos de Catalão (GO) e Tapira (MG), Brasil. *Geochimica Brasiliensis* 20 (2). <https://geobrasiliensis.org.br/geobrasiliensis/article/view/243>.

Conceição, F. T., P. M. Vasconcelos, L. H. Godoy, G. R. B. Navarro, C. C. Montibeller, and D.S. Sardinha. 2022. Water/Rock Interactions, Chemical Weathering and Erosion, and

Supergene Enrichment in the Tapira and Catalão I alkaline-carbonatite complexes, Brazil. *Journal of Geochemical Exploration* 237 (June):106999. <https://doi.org/10.1016/j.gexplo.2022.106999>.

Ellis, D. V., and J. M. Singer, eds. 2008. *Well Logging for Earth Scientists*: 2nd ed. corrected printing. Dordrecht: Springer Netherlands. 708 pp. <https://doi.org/10.1007/978-1-4020-4602-5>.

Fonseca, L. 2014. Avaliação de métodos de perfilagem geofísica na pesquisa de minério de ferro – Estudo de caso: definição de contatos litológicos na mina de Capanema, MG. Master's thesis, Universidade Federal de Ouro Preto, Ouro Preto, MG, Brazil. 125 pp. <http://www.repositorio.ufop.br/handle/123456789/4226>.

Gasper, G. O., O. S. Ayodeji, P. Salvadoretti, and J. F. C. L. Costa. 2015. Determination of Coal Seam Thickness in Blast Holes Utilizing Geophysical Well Logging Data and Its Use in Short Term Mine Planning. In 14th International Congress of the Brazilian Geophysical Society & EXPOGEF, Rio de Janeiro, Brazil, 3-6 August 2015, 492–95. SEG Global Meeting Abstracts. Brazilian Geophysical Society. <https://doi.org/10.1190/sbgf2015-097>.

Gibson, S. A., R. N. Thompson, A. P. Dickin, and O. H. Leonardos. 1995. High-Ti and Low-Ti Mafic Potassic Magmas: Key to Plume-Lithosphere Interactions and Continental Flood-Basalt Genesis. *Earth and Planetary Science Letters* 136 (3): 149–65. [https://doi.org/10.1016/0012-821X\(95\)00179-G](https://doi.org/10.1016/0012-821X(95)00179-G).

Gomes, C. B. 2020. Os Carbonatitos Cretácicos da Plataforma Brasileira e Suas Principais Características. São Paulo, Brazil: Instituto de Geociências da USP. 253 pp. <https://doi.org/10.11606/9786586403008>.

Gorelik, B., G. O. Gasper, P. Salvadoretti, D. S. Q. Libardi, T. Almeida, and J. F. C. L. Costa. 2019. Avaliação do uso da perfilagem geofísica para reconhecimento e determinação de espessuras de camadas de carvão em depósitos do Rio Grande do Sul. *Geosciences = Geociências* 38 (1): 157–70. <https://doi.org/10.5016/geociencias.v38i1.12525>.

Hajnal, Z., E. Takacs, B. Pandit, and I. R. Annesley. 2015. Uranium Mineralization Indicators from Seismic and Well Log Data in the Shea Creek Area at the Southern Margin of the Carswell Impact Structure, Athabasca Basin, Canada. *Geophysical Prospecting* 63 (4-Hard Rock Seismic imaging): 861–80. <https://doi.org/10.1111/1365-2478.12274>.

Horrocks, T., E.-J. Holden, and D. Wedge. 2015. Evaluation of Automated Lithology Classification Architectures Using Highly-Sampled Wireline Logs for Coal Exploration. *Computers & Geosciences* 83 (October): 209–218. <https://doi.org/10.1016/j.cageo.2015.07.013>.

Howell, E. P., O. J. Gant Jr., and Terry J. Crebs. 1980. Slim Hole Logging and Analysis for Uranium Exploration. *Journal of Petroleum Technology* 32 (07): 1144–50.

<https://doi.org/10.2118/7434-PA>.

Kowalski, J., and W. H. Fertl. 1977. Application of Geophysical Well Logging to Coal Mining Operations. *Energy Sources* 3 (2): 133–47. <https://doi.org/10.1080/00908317708945975>.

Lipton, I. T. 2001. Measurement of Bulk Density for Resource Estimation. In *Mineral Resource and Ore Reserve Estimation – The AusIMM Guide to Good Practice*, Monograph 23, edited by A. C. Edwards, 57–66. Melbourne, Australia: Australasian Institute of Mining and Metallurgy.

Lipton, I. T., and J. A. Horton. 2014. Measurement of Bulk Density for Resource Estimation – Methods, Guidelines and Quality Control. In *Mineral Resource and Ore Reserve Estimation – The AusIMM Guide to Good Practice*, 2nd edition. Monograph 30, 97–108. Melbourne, Australia: Australasian Institute of Mining and Metallurgy.

Luiz, J. G. 2013. *Geofísica na prospecção mineral: Guia para aplicação*. Séries de Geofísica. Rio de Janeiro, RJ, Brazil: SBGf. 108 pp.

Mussett, A. E., and M. A. Khan. 2000. *Looking into the Earth: An Introduction to Geological Geophysics*. Cambridge: Cambridge Univ. Press. <https://doi.org/10.1017/CBO9780511810305>.

Nery, G. G. 2013. *Perfilagem Geofísica em Poço Aberto: Fundamentos básicos com ênfase em petróleo*. Rio de Janeiro, RJ, Brazil: SBGf. 222 pp. https://sbgf.org.br/mysbgf/images/Girao_previa.pdf.

Novaes, L. C. 2018. *Processos metalogenéticos associados a complexos alcalino-carbonatíticos da Província Ígnea Alto Paranaíba, Sudeste Brasileiro [Metallogenetic Processes Associated with Alkaline-Carbonatite Complexes of the Alto Paranaíba Igneous Province, Southeastern Brazil]*. Undergraduate thesis, Universidade Federal do Paraná, Curitiba, Brazil. 92 pp.

Oliveira, I. W. B., L. L. B. Sachs, V. A. Silva, and I. H. Batista. 2004. Geological Map of Brazil at 1:1000000 Scale – Sheet SE-23 Belo Horizonte. Geographic Information System (GIS). Scale 1:1000000. Brasília, Brazil: CPRM – Geological Survey of Brazil. <https://rigeo.sgb.gov.br/handle/doc/4993>.

Oliveira, L. J. 2005. Avaliação do uso da perfilagem geofísica para obtenção de informações secundárias para utilização em co-estimativas de variáveis geológico-mineiras. Master's thesis, Universidade Federal do Rio Grande do Sul, Porto Alegre, Brazil. 164 pp. <https://lume.ufrgs.br/handle/10183/5857>.

Penney, R., C. Ames, D. Quinn, and A. Ross. 2012. Determining Uranium Concentration in Boreholes Using Wireline Logging Techniques: Comparison of Gamma Logging with Prompt Fission Neutron Technology (PFN). *Applied Earth Science* 121 (2): 89–95.

<https://doi.org/10.1179/1743275812Y.0000000022>.

Pereira, W. R., D. U. Carlos, and M. A. S. Braga. 2016a. Density Correction for Geophysical Well Logging inside Drilling Rods. *Revista Brasileira de Geofísica* 33 (4). <https://doi.org/10.22564/rbgf.v33i4.755>.

Pereira, W. R., D. U. Carlos, M. A. S. Braga, and H. F. Galbiatti. 2016b. Evaluation of Gamma-Gamma Well Logging Data Applied to Iron Ore Exploration – Vale Geophysical Well Logging Test Facility. *Revista Brasileira de Geofísica* 34 (2). <https://doi.org/10.22564/rbgf.v34i2.796>.

Prieto, R. F. 2021. Aplicação de aprendizado supervisionado em dados de perfilagem geofísica para a classificação automatizada de litotipos na exploração de minério de ferro em Carajás. Master's thesis, Universidade de São Paulo. São Paulo, Brazil. <https://doi.org/10.11606/D.14.2021.tde-22082021-145637>.

Reis, C., C. Arroyo, A. Curi, and M. Zangrandi. 2021. Impact of Bulk Density Estimation in Mine Planning. *Mining Technology* 130 (1): 60–65. <https://doi.org/10.1080/25726668.2021.1876481>.

Rider, M. H., and M. Kennedy. 2011. *The Geological Interpretation of Well Logs*: 3rd ed. Aberdeen, Scotland: Rider-French Consulting Limited. 432 pp.

Silva, C. Z. 2010. Uso da perfilagem geofísica gama-gama e gama natural na mineração: suas aplicações, vantagens e limitações. Undergraduate thesis, Universidade Federal do Rio Grande do Sul, Porto Alegre, Brazil. 35pp. <https://lume.ufrgs.br/handle/10183/28722>.

Silva, L. M. C., and J. G. Luiz. 1995. *Geofísica de prospecção*. 3rd ed. Vol. 1. 1 vols. Belém, Brazil: Universidade Federal do Pará: Cejup.

Sonoki, I. K., and G. M. Garda. 1988. Idades K-Ar de rochas alcalinas do Brasil meridional e Paraguai oriental: compilação e adaptação às novas constantes de decaimento. *Boletim IG-USP. Série Científica* 19 (January):63–85. <https://doi.org/10.11606/issn.2316-8986.v19i0p63-85>.

Souza, V., P. Salvadoretti, J. F. C. L. Costa, F. Beretta, J. C. Koppe, G. A. Bastiani, J. A. Carvalho Júnior, and A. Grigorieff. 2010. Estimativa de qualidade de carvão por meio de perfilagem geofísica de gama natural e resistividade. *REM: Revista Escola de Minas* 63, nº 4: 653-660. <https://doi.org/10.1590/S0370-44672010000400009>.

Webber, T. 2008. Estimativa de qualidade de carvão usando krigagem dos indicadores aplicados a dados obtidos por perfilagem geofísica. Master's thesis, Universidade Federal do Rio Grande do Sul, Porto Alegre, Brazil. 286 pp. <https://lume.ufrgs.br/handle/10183/13559>.

Webber, T., J. F. C. L. Costa, and P. Salvadoretti. 2013. Using Borehole Geophysical Data as

Soft Information in Indicator Kriging for Coal Quality Estimation. *International Journal of Coal Geology*, Special issue on geostatistical and spatiotemporal modeling of coal resources, 112 (June):67–75. <https://doi.org/10.1016/j.coal.2012.11.005>.

Williams, J. H., and C. D. Johnson. 2004. Acoustic and Optical Borehole-Wall Imaging for Fractured-Rock Aquifer Studies. *Journal of Applied Geophysics*, Non-Petroleum Applications of Borehole Geophysics, 55 (1): 151–59. <https://doi.org/10.1016/j.jappgeo.2003.06.009>.

Wynn, J. 1996. Geophysics Applied to Phosphate Exploration in Northern Saudi Arabia. In SEG Technical Program Expanded Abstracts 1996, 600–602. SEG Technical Program Expanded Abstracts. Society of Exploration Geophysicists. <https://doi.org/10.1190/1.1826715>.

Paula, C.A.: field data acquisition, analysis, data interpretation, manuscript preparation, writing, editing and review; **Carvalho, C.A.**: field data acquisition, analysis, data interpretation; **Braga, M.A.**: field data acquisition, analysis and data interpretation, theoretical support, writing review; **Dal' Bó, P.F.**: theoretical support, writing review; **Louback, V.S.**: theoretical support, writing review; **Salvadoretti, P.**: field data acquisition, theoretical support; **Vieira, L.B., Paes, L.C.O., Gonçalves, R.B.O., Feuchard, L.D. and Santos, K.P.**: field data acquisition.

Received on January 23, 2025 / Accepted on August 27, 2025